Multi-omics Analysis of Redox Imbalance-Related Mild Health Problems in Monkeys

Fumie Hamano
The University of Tokyo
Suzumi M Tokuoka
The University of Tokyo
Megumi Ishibashi
Thermo Fisher Scientific K. K
Yasuto Yokoi
Mitsui Knowledge Industry Co., Ltd. Atago Green Hills MORI Tower
Dieter M Tourlousse
Advanced Industrial Science and Technology (AIST)
Yoshihiro Kita
The University of Tokyo
Yuji Sekiguchi
Advanced Industrial Science and Technology (AIST)
Hiroyuki Yasui
Kyoto Pharmaceutical University
Takao Shimizu
The University of Tokyo
Yoshiya Oda (yoda@m.u-tokyo.ac.jp)
The University of Tokyo

Research Article

Keywords: definitive diseases, metabolomics data, multi-omics analysis, redox imbalance-related mild health problems

Posted Date: April 23rd, 2021

DOI: https://doi.org/10.21203/rs.3.rs-453434/v1

Abstract

Certain symptoms associated with mild sickness and lethargy have not been categorized as definitive diseases. Confirming such symptoms in captive monkeys (*Macaca fascicularis*) can be difficult; however, it is possible to observe and analyze their feces. Even among monkeys that are housed under carefully monitored conditions, some monkeys occasionally have poor stool conditions. In this study, we investigated the relationship between stool state and various omics data by considering objective and quantitative values of stool water content as a phenotype for analysis. By examining the food intake of the monkeys, the stool and urine they expel, and the plasma circulating in their bodies, we attempted to obtain a comprehensive understanding of the health status of a single individual and understand its relationship with stool condition. Our metabolomics data strongly suggested an association between lipids and stool water content. Lipidomic analysis revealed the involvement of saturated and oxidized fatty acids, metallomics revealed the contribution of selenium (a bio-essential trace element), and intestinal microbiota analysis revealed the association of several bacterial species with the stool water content. Taken together, these results suggest that selenium-induced disturbance in redox balance may cause minor health problems.

Introduction

Living a healthy life and reaching old age without suffering and disease are common aspirations of human society. However, there are many diseases to be overcome, including widely recognized diseases, such as cancer, dementia, and infectious diseases, as well as diseases that cannot be diagnosed using conventional techniques, despite the presence of clinically evident symptoms. The pre-symptomatic state of diseases, which is somewhere between health and illness, is also drawing attention. Various disease models are used to elucidate disease mechanisms and to develop diagnostic and therapeutic strategies. In vitro experiments using cell lines are relatively inexpensive and suitable for high-throughput screening, but there exists a large gap between in vitro experiments and phenomena observed in the body in vivo. Mice are widely used as experimental models; however, there are significant differences in the biology and behavior of rodents and humans. For example, mice do not naturally develop aging-related diseases such as atherosclerosis and diabetes, partly due to their short lifespan[1,2]. Therefore, non-human primates (NHPs) could serve as interesting experimental models as they are quite close to humans in terms of evolutionary distance[3]. Unlike research on humans, research on NHPs allows for complete control over housing, environment, diet, and behavior.

A survey investigating the experiences of veterinary clinicians working on primate diarrhea in 1981 revealed the incidence of diarrhea in 13,385 monkeys to be 10.6%[4]; however, a 2018 study reported that diarrhea occurs in 3.6–31.6% of monkeys housed under conditions of captivity[5]. If symptoms do not improve, it may lead to death or engender the need for euthanasia. Previous studies have repeatedly shown that both personality and psychological stressors can serve as predictors of gastrointestinal diseases and chronic diarrhea[5]. In general, the risk of diarrhea is higher when one is nervous, introverted,

and/or anxious. While certain stressful environments increase the risk of chronic diarrhea, the relative impact of these stressors is believed to be highly dependent on the animal's personality[5]. In humans, diarrhea is one of the most common functional bowel diseases, affecting 8–20% of the general population worldwide. In particular, irritable bowel syndrome (IBS), with diarrhea as a typical symptom, appeared to be associated with high psychosocial stress and low quality of life and work productivity[6,7]. However, the mechanisms underlying the development of IBS are largely unknown. Chronic psychological stress is thought to play an important role in the onset and worsening of symptoms of functional bowel disease[7,8].

To study complex biological processes in a comprehensive manner, an integrated approach that involves omics analyses on different samples, such as blood and urine, to reveal the interrelationships between the biomolecules and their functions may provide a more thorough understanding of health and disease[9–12]. In multi-omics, a correlation is identified between a vast array of molecular profile information and the disease status. Therefore, it is important to evaluate the phenotypes of diseases as continuous and objective quantitative values. In this study, stool water content was considered as a phenotype[13,14], and multi-omics data pertaining to blood, urine, feces, and food were obtained from monkeys housed in a controlled environment.

Results

The amount of water contained in each fecal sample is shown in Supplementary Table S1. The values were obtained by weighing about 50 mg of stool and measuring the dry weight after drying it for 24 h. The feces of the five monkeys with star marks had high water content (comprising the top 6) and were visually observed to be soft stools, suggesting that the water content in the feces reflects the stool condition. The stool water content was handled as a quantitative and an objective phenotype, and an association was investigated with the following omics data.

Metabolomics

Using untargeted metabolomics analyses, we detected 899 peaks in plasma (Supplementary Table S2), 2920 peaks in urine (Supplementary Table S3), and 3125 peaks in feces (Supplementary Table S4). As the number of monkeys in this study was small (n = 20), we excluded peaks with missing values (below the detection limit). The number of peaks with significant correlations ($p < 0.05$) included 85 peaks for plasma metabolites, 267 peaks for urinary metabolites, and 1347 peaks for fecal metabolites. Among them, the metabolites with particularly strong correlations (peaks with a strong correlation (± 0.8)) with the stool water content, were examined based on Pearson's correlation coefficient. Such metabolites were not found in plasma or urine. However, 18 metabolites in stool had a positive correlation, and 92 had a negative correlation with the stool water content. When the strength of the correlation was expanded to ± 0.7, 392 peaks were correlated (along with three in urine and two in plasma). We attempted to identify these metabolites using the "LC-MS Search" function (https://hmdb.ca/spectra/ms/search) of The

Human Metabolome Database (HMDB) with accurate mass number. We speculated 982 metabolite names (HMDB ID numbers), including redundancies such as structural and stereoisomers (Supplementary Table S5). As we did not use any standard metabolites for confirmation, it was difficult to specifically identify the metabolites, and some of the metabolites were considered misidentified. However, while misidentifications are likely to occur randomly, correct identifications were made by annotating the characteristics of candidate metabolites to identify the metabolic pathways/networks most likely to be affected by these metabolites and the population of metabolites with common characteristics[15–18]. Therefore, we used this information to perform an analysis using the Enrichment Analysis function of MetaboAnalyst 5.0 (https://www.metaboanalyst.ca/). As shown in Supplementary Fig. S1, more than half (53.4%) of the metabolites whose structures could be estimated by HMDB were lipid-related metabolites. Hence, we focused our subsequent analysis on lipids.

Fatty Acid Analysis

To examine the lipids in more detail, the basic structural units of lipids and fatty acids were analyzed using GC. Free fatty acids and fatty acids covalently bound to-cholesterol and -glycerol skeletons via ester bonds were hydrolyzed, so the total amount of fatty acids could be measured. The results are shown in Fig. 1. The most common fatty acid in the feed (orange bars) was C18:2n-6 (54.5%), followed by C18:1n-9 (20.4%), and these two accounted for approximately 75% of the total fatty acid content. Many of the unsaturated fatty acids found in the diet were reduced to the saturated form in the feces (blue bars), except for the C18 series, whose levels increased in the feces.

As shown in Fig. 2, the correlation of fatty acids present in feces with stool water content was determined. Two fatty acids, C18:2n-6 and C18:1n-9, were positively correlated with the stool water content. These two fatty acids were abundant in the diet. Thus, in monkeys with defective intestinal absorption, the composition of the food may be strongly reflected in their feces. As the absorption of water in the intestinal tract as well as the ingredients of the food are decreased, the amount of water in the stool is increased. Saturated fatty acids showed a strong negative correlation with stool water content (less than − 0.8). Although the origin of the saturated fatty acids is unknown, the stool with more saturated fatty acids had lower stool water content. There was no significant correlation between plasma fatty acids and stool water content (Supplementary Table S6). The levels of urinary fatty acids were not measured because the quantitative sensitivity of the assay was insufficient for the 200 µL of urine obtained in this study.

Lipidomics

Untargeted lipidomic analyses were conducted to determine the source of saturated fatty acids in the stool. As only LipidSearch[19,20] was used as an analysis method and no verification using standard products was conducted, there is a possibility of false identifications. However, we decided to focus on lipid subclasses, rather than the individual molecules identified.

We performed lipidomic analyses on monkey feed and identified 361 lipid components (Supplementary Table S7), as shown in Fig. 3. More molecular species belonged to TG than the other lipids, but the distribution of other lipids seemed to be relatively well balanced. Subsequently, we conducted fecal lipidomics, and 844 lipids were identified (Supplementary Table S8). Figure 4**(a)** shows the distribution of lipid components in the stool. The TG abundant in the food decreased significantly, and the PE content increased. The constituents in the stool are difficult to interpret because they are a mixture of undigested food residues from the intestinal tract and the molecules produced by intestinal bacteria. The presence of PE as a major phospholipid in feces confirms the fact that these molecules are more abundant in bacteria than in mammals. Fecal lipids with a positive correlation ($p < 0.05$) with stool water content are shown in Fig. 4**(b)**. PA, PEt, and PMe were characteristic minor components in the stool. Figure 4**(c)** shows the lipids with a negative correlation. As the amount of water absorbed from the intestine decreases (amount of water in the stool increases), the amount of PE absorbed from the intestine may also decrease. However, if the decrease in absorption is not limited to PE, then the level of PE produced by the bacteria may reduce as the stool water content increases.

The lipids in the stool that were correlated with water content were not very strongly correlated with each other (positive and negative correlations of approximately ± 0.5). Therefore, plasma lipidomic analysis was performed to identify 711 lipids, which were less than the molecular species identified in fecal lipidomic analysis (Supplementary Table S9). The distribution of plasma lipid species is shown in Fig. 5**(a)**. The TG component abundant in the food, was also abundant in the plasma, which was very different from the lipid component in the stool. In addition, the percentage of glycerophospholipids, including PC and PE, increased in the plasma compared with that in the food. Five plasma lipids (two each of PC and PE, and one of PG) were positively correlated with stool water content, and the correlation was not strong ($0.5 < r < 0.6$). However, there were 239 lipids with a negative correlation ($p < 0.05$), and their distribution is shown in Fig. 5**(b)**.

Nineteen of the negatively correlated plasma lipids exhibited correlation coefficients of -0.7 or lower with the stool water content, which was much higher than that observed for lipids in the stool (Supplementary Table S8). Of these, 10 were TGs, and the abundance of TGs was also characteristic in Fig. 5**(b)**. LPC also tended to be abundant as a plasma lipid with negative correlation, and four of them exhibited correlation coefficients of -0.7 or lower with the stool water content.

Lipidomic analysis was also carried out on urine samples. We identified 566 lipids in urine, which were fewer than the lipids found in stool and plasma, but more than that in food (Supplementary Table S10). As shown in Fig. 6**(a)**, the relatively high number of TG species followed the same trend as in plasma, but the higher number of PEs than of PCs was more pronounced in urine than in stool. Above all, the very high percentage of sphingolipids is probably a characteristic of urinary lipids. There were 42 urinary lipids that were positively correlated with the stool water content. The correlation coefficients with stool water content were all less than 0.6 and were not as high as those of plasma lipids. However, it is noteworthy that the correlations were positive, unlike those of plasma and feces. Most of the urinary lipids with a positive correlation were sphingolipids. Although TG and PE were also common as urinary lipids, they did

not correlate well with the stool water content. Both plasma TG and PE have been found to be inversely correlated with the stool water content. Only one type of lipid, PS, had a negative correlation with the stool water content, and the correlation coefficient was − 0.45 (not a strong correlation).

Lipid Mediator Analysis

In addition to general lipidomic analysis, we also measured the levels of fatty acid-derived lipid mediators and their related metabolites (FA metabolites) for functional analysis of the feces; 14 FA metabolites in the stool (Supplementary Table S11) and two FA metabolites in plasma (Supplementary Table S12) were positively correlated with stool water content (only oxidized lipids that were above the lower limit of quantification). Among them, six FA metabolites with relatively high correlation coefficients (0.6 or higher) are shown in Supplementary Table S13. In addition, urinary FA metabolites, which were detected in 20 animals, did not correlate with the stool water content (Supplementary Table S14).

The precursor of these oxidized fatty acids (excluding 13-HOTrE) was linoleic acid (LA, C18:2n-6). As shown in Fig. 1, LA accounted for more than half of these precursors in food, suggesting that they were modified by oxidizing enzymes such as lipoxygenases (LOX) and cytochrome P450 (CYP)[21,22]. C18:2n-6, the precursor of two FA metabolites in plasma (9-KODE and 9-HpODE), which were positively correlated, was also most abundant in the food. These oxidized fatty acids in stool, particularly 13-HpODE, are known to promote intestinal inflammation[23,24], may affect the intestines, and cause soft stools, even if they do not lead to a specific disease. However, due to oxidative stress in the body, the production of 13-HpODE and other substances may have increased, causing inflammation of the intestines and poor food absorption. Two of the oxidized fatty acids in plasma also correlated with the stool water content, suggesting that monkeys with soft stools may have increased oxidation not only in their stool but also in their blood.

Metallomic Analysis

In general, the concentration of ions in the gastrointestinal tract changes the osmotic pressure in the lumen, which in turn affects stool water content. Therefore, the trace elements, including metallic elements that constitute inorganic substances in feces, blood, and urine, were also measured. The correlations with stool water content are shown in Fig. 7 (and Supplementary Table S15). The only element in plasma with correlation coefficients higher than 0.5 or lower than − 0.5 was selenium (Se), which showed a negative correlation with the stool water content (-0.637, $p = 0.0025$), and no such correlation was found in stool or urine. Although Se is an essential element and has antioxidant properties, it is incorporated into proteins as selenocysteine in vivo and is predominantly found as selenoprotein P in plasma[25–27]. Glutathione peroxidase (GPx), one of the selenoproteins, is an enzyme that plays an important role in the reduction of lipid peroxides.

In this case, oxidized fatty acids in plasma and stool (digestive tract) increase (oxidation is enhanced). This redox imbalance in the body may lead to poor health (soft stools). Metallomic analysis of trace

elements in the food revealed that all the elements shown in Fig. 7 were present in the food (Supplementary Table S16). However, recent studies have shown that Se, an essential trace element for living organisms, is stored in intestinal bacteria and is utilized by the host as and when needed[28]. Therefore, we investigated the intestinal bacteria from feces.

Microbiota Analysis

Based on microbiota profiling by 16S rRNA gene amplicon sequencing, we further assessed the correlation between the abundance of amplicon sequence variants (ASVs) and the stool water content. For this analysis, we considered ASVs that were detected in the feces of at least half the monkeys (based on the mean of rarified ASV tables of duplicate measurements per monkey, see Methods). This subset of ASVs (n = 405) accounted for 91.7 ± 2.2% (mean and standard deviation) of total abundances across samples/monkeys. Using Spearman's correlations to identify monotonic associations, we recovered a total of 60 ASVs that were significantly (adjusted P-value of < 0.1) correlated with the stool water content (Fig. 8a and Supplementary Fig. S2).

Within the family Lachnospiraceae, the abundance of ASVs belonging to multiple genera, including *Blautia*, *Roseburia*, and *Dorea*, was positively correlated with the stool water content and increased up to an order of magnitude in abundance (as a percentage of the total community) across the range of the stool water contents evaluated. Other ASVs that were positively correlated with water content included ASVs from members of the genera *Holdemanella* and *Faecalibacillus* (family *Erysipelotrichaceae)*, and *Prevotella (*family *Prevotellaceae)*. For the family *Ruminococcaceae*, correlation coefficients had varying signs across ASVs, with both significant positive and negative associations with water content. Many ASVs that negatively correlated with water content could be identified only at higher taxonomic levels. Based on the ASV table collated at the family level (that is, by summing ASV abundances within families), *Lachnospiraceae* was significantly positively correlated with the stool water content, consistent with the positive correlations for a considerable number of ASVs within this family, whereas *Ruminococcaceae* was negatively associated with the stool water content, although the correlation was not significant (Supplementary Fig. S3).

In line with the mounting evidence that the families *Lachnospiraceae* and *Ruminococcaceae* play an important, potentially dual (beneficial and detrimental) role in the development of intra- and extra-intestinal diseases[29–31], correlation analysis also suggested an association between both families and mild health conditions in our monkeys. Although the genera *Dorea* and *Blautia* within the family *Lachnospiraceae* are generally considered members of a healthy gut microflora, increased abundance of *Dorea* in diarrheic Japanese individuals has been reported[32], whereas enrichment of *Blautia* has been shown in the stool of individuals with self-reported bowel symptoms[33]. Further, the family *Erysipelotrichaceae* has been linked to inflammation-related gastrointestinal diseases[34], and Nakajima *et al.*[35] reported a positive correlation between the genus *Holdemanella* and diarrhea in patients with type 2 diabetes mellitus. In foals, Schoster *et al.*[36] reported underrepresentation of the family *Ruminococcaceae*

and *Lachnospiraceae* in fecal samples of diarrheic subjects. Although we also found a significant decrease in some ASVs within the family *Ruminococcaceae* with increasing stool water content, other *Ruminococcaceae*-related ASVs showed an opposite trend.

Taken together, fecal microbiota analyses suggested several microbial signatures that may be indicative of intestinal dysbiosis in monkeys with elevated stool water content. However, the possible role(s) of these bacteria in modulating host physiology, and especially redox balance, remains to be elucidated.

Discussion

One of the bottlenecks of using multi-omics analyses to analyze individuals subjects (humans and animals) is the handling of phenotypes. Especially in the case of non-defined diseases, there are only qualitative indexes, which do not fit well with quantitative omics data. In this study, we obtained continuous quantitative data using the water content in stool as a phenotype for reflecting the health status of monkeys, when monkeys have been housed for a long time under the same conditions and controlled for infection. In general, saturated fatty acids are considered harmful for the body[37–39]. However, the observation that the amount of saturated fatty acids in the stool decreased as the stool became softer (as the stool water content increased) was unexpected. It has also been reported that an increase in saturated fatty acid levels in the lumen of the colon improves gastrointestinal motility[40]. Fatty acids other than free fatty acids are often stored as TG[41]. The molecular species that correlated strongly (inverse correlation) with stool water content were saturated fatty acids in stool, followed by TG in plasma. In other words, the higher the stool water content, the lower the plasma TG level. It has been reported that plasma TG levels and oxidative status in plasma are inversely correlated[42,43]. This means that the blood of monkeys with soft stools may be in an oxidative status. In our data, plasma selenium was also inversely correlated with stool water content. Additionally, the level of selenium, which has antioxidant properties, was decreased in soft stools along with an increase in oxidized fatty acid levels, suggesting that blood may be inclined to the oxidative status. Selenoprotein P is an enzyme involved in the metabolic pathway of PE[44]. Like selenium, many plasma PEs (major phospholipid in bacteria) are inversely correlated with stool water content, and PEs are also more pronounced in the stool. Furthermore, phospholipase D is activated by reactive oxygen species[45,46], and it is known to produce PA as well as PEt[47,48]. Therefore, in soft stools, PA and PEt levels may have increased due to the components of the stool tending to the oxidative status. In diabetic nephropathy, oxidative stress increases sphingolipid levels[49], and sphingolipids have been reported to regulate redox homeostasis in chronic kidney disease[50]. In our study, urinary sphingolipid levels increased with soft stools, suggesting that the urinary condition tended to be oxidized in soft stools. Many studies have reported that oxidative stress is involved in inflammation and affects gut health, and the results of this study confirm previous data[51,52].

Although there are some phenomena that cannot be directly explained by the redox state, for example, the concentration of LPC in the plasma (strongly inversely correlated with soft stool) increases in certain inflammatory conditions, but recently there have been reports that a decrease in plasma LPC

concentration worsens the disease[53]. However, the mechanism of action of some lipids is complex, and not all of them can be explained. In this study, intestinal bacteria were also found to be associated with soft stools, but the detailed involvement of intestinal bacteria in the mechanism of action is unknown. However, by systematically examining the food that enters the body, the feces and urine that leave the body, and the plasma that circulates in the body of a single individual, it becomes possible to evaluate what is happening inside the body. In this study, we only collected samples at one point in time, but by examining changes over time, we may be able to construct a hypothesis about what is happening inside the body.

Methods

Monkey (*Macaca fascicularis*) samples (plasma, urine, and stool) from 20 male animals (aged 3 years 10 months to 6 years 5 months), housed for more than 8 months under the same conditions, were obtained from LSI Medience Co. (Tokyo, Japan) after review by the Animal Experimentation Committee, and approval by the Director of the Testing and Research Center in LSI Medience Co. (Approval No. 2018 – 1071). The monkeys were housed with the lighting turned on from 7:00 to 19:00 and turned off at night. The cages were cleaned once a day. The monkeys were fed 100 g of solid feed (CLEA Old World Monkey Diet CMK-2, CLEA Japan Inc., Tokyo) once a day. Filtered (5 μm filter) and UV irradiated tap water was provided as drinking water. Monkeys have a habit of urinating when the lights are turned on in the morning, so urine was collected early in the morning by placing a urine collection tray in the home cage and lighting up the animal room. Regarding stool collection, since we did not know when the monkeys would defecate, a tray for feces was placed in the home cage, and the animal caretakers collected the stool into a plastic tube as soon as they found one. On the same day as urine collection, approximately 5 mL blood was drawn in a tube with EDTA-2K and centrifuged (1750 x *g*, 10 min, 4°C) to obtain approximately 2 mL plasma. All samples were frozen and stored in the − 80°C freezer at LSI Medience immediately after collection and kept on dry ice during transport.

Sample preparation

To carry out targeted lipidomics/fatty acid analysis by Gas Chromatography with Flame Ionization Detection (GC-FID), 50 μL plasma samples and 20 mg wet weight of feces and feed (The feces and feed were dissolved while dipped in the sonication bath, and the feed was fully pulverized with a stainless-steel crusher) were derivatized using the Fatty Acid Methylation Kit (Nacalai Tesque, Tokyo) with C23:0 fatty acid solution (n-Tricosanoic acid, Sigma-Aldrich) as an internal standard.

For untargeted lipidomics by LC/MS, 20 μL of plasma was combined with 180 μL of methanol, vortexed, and centrifuged to collect the supernatant. The supernatant was further diluted three times with methanol for the analysis. Urine lipids were recovered from the organic layer of 300 μL urine using the Bligh & Dyer method, followed by evaporation of the organic solvent, and resuspension of the residuals in 60 μL methanol for measurement. About 20 mg of feces was weighed (wet weight) and mixed with 20 μL water, and kept on ice. After vortexing, 180 μL methanol was added, and the mixture was stirred in an ultrasonic

bath with ice cooling. After centrifugation, the supernatant was diluted four times with methanol and used to measure phospholipids. Twenty milligrams of feed was ground and extracted with 500 µL methanol. After centrifugation, the supernatant was collected and diluted with methanol to 5 mg/mL.

For targeted lipidomics by LC/MS, solid-phase extraction (SPE) was performed as described previously with some modifications[54]. 200 µL of plasma was combined with 0.8 mL of methanol and mixed with internal standards (18 heavy water labelled components) and centrifuged to collect the supernatant. The supernatant was then purified using an Oasis HLB cartridge (10mg, Waters, Milford, MA) and eluted with 200 µL of 0.2% formic acid in methanol. The solvent was evaporated by rotary evaporator and resuspended in 50 µL of methanol for measurement. Four hundred µL of urine was centrifuged after mixing with 800 µL of methanol and internal standards, and the supernatant was applied to Oasis HLB cartridge, as mentioned above for plasma. The eluate was measured. About 150 mg of feces was measured as wet weight, and 300 µL of water was added on ice and mixed well. Subsequently, 1.2 mL of methanol and internal standards were added, mixed in an ultrasonic bath while chilled/ The supernatant was purified using an Oasis HLB cartridge as mentioned above for plasma samples, and eluted with 200 µL of 0.2% formic acid in methanol. The eluate was analyzed by LC/MS.

To carry out untargeted metabolomics for hydrophilic metabolites analysis by LC/MS, 560 µL methanol was added to 140 µL plasma and vortexed, centrifuged, and 600 µL supernatant was concentrated in a rotary evaporator and resuspended in 100 µL methanol for measurement. For urine, the upper layer (aqueous phase) of the Bligh & Dyer extraction with 300 uL urine was dried up by a rotary evaporator and resuspended in 100 µL methanol for measurement. For feces, about 20 mg wet weight of feces was suspended in 20 µL water on ice, followed by the addition of 180 µL methanol, and mixed in an ultrasonic bath while chilled. After centrifugation, the supernatant was diluted four times with methanol and measured. The 20 mg food was smashed, mixed well with 800 µL methanol, centrifuged to collect the supernatant, and then diluted 10-fold with methanol for measurement.

For trace element measurements, each sample (50 mg for feed samples, 50 µL each for plasma samples, 50 µL each for urine samples, and the entire volume of each feces sample) was placed into a 50-mL tall beaker and heated on hotplates to 150°C. After 3 minutes, 2 mL 60% (v/v) nitric acid (HNO_3 for poisonous metal determination; Kanto Chemical, Tokyo, Japan) was added, followed 3 minutes later by 2 mL 60% (v/v) perchloric acid ($HClO_4$ for poisonous metal determination; Kishida Chemical, Osaka, Japan), and 3 minutes later by 2 mL 30% (v/v) hydrogen peroxide (H_2O_2 for atomic absorption spectrochemical analysis; Kishida Chemical, Osaka, Japan). This process was repeated three times, and if any brownish residue remained, it was repeated further until the sample was completely white. Thus, ashing was continued until the residual material at the bottom of the tall beaker turned completely white. After the sample was cooled to room temperature, 5 mL (feed, plasma, and urine) or 10 mL (feces) of 5% (v/v) nitric acid was added and allowed to stand at room temperature for 24 hours to completely dissolve any remaining material. Then, 5 µL (feed, plasma, and urine) or 10 µL (feces) of 1 µg/mL indium (In) was added as an internal standard solution, mixed well, and each sample solution was transferred to a

polycarbonate cup for ICP-MS measurement. Tall beakers and sample cups were previously soaked in 1% nitric acid for at least 3 days, washed with ultrapure water, and dried.

For 16S rRNA gene amplicon library construction and sequencing, extraction of DNA from fecal samples (approximately 200 mg of biomass per sample) was performed using the ISOSPIN Fecal DNA kit (Nippon Gene Co., Ltd.), according to manufacturer's instructions. For cell lysis, three rounds (1 min each) of bead beating were performed using the FastPrep-24 instrument (MP Biomedicals) at a speed of 6 m/s. DNA concentrations were measured with the Quant-iT PicoGreen dsDNA Assay Kit using a Qubit fluorometer (both from Invitrogen). Amplicon sequencing libraries were prepared by two-step tailed polymerase chain reaction (PCR) following Illumina's "16S Metagenomic Sequencing Library Preparation" protocol. In the first round of PCRs, the V4 hypervariable region of the 16S rRNA gene was amplified using primers 515F (5'-GTGYCAGCMGCCGCGGTAA-3') [55] and 806R (5'-GGACTACNVGGGTWTCTAAT-3')[56]; primers contained appropriate 5'-end adapters required for indexing in the second round of PCR. Reactions (20 µL) consisted of 1 × KAPA HiFi HotStart ReadyMix (Roche), 500 nM each of forward and reverse primer, and 5 ng template DNA. Thermal cycling conditions were as follows: 95°C for 3 min; followed by 18 cycles of 95°C for 30 s, 50°C for 30 s and 72°C for 30 s; and finally 72°C for 5 min. PCR products were purified using the Agencourt AMPure XP system (1× volume of AMPure beads) and eluted in 50 µL 10 mM Tris-HCl buffer (pH 8.0). The second round of PCRs (30 µL) contained 1 × KAPA HiFi HotStart ReadyMix, 3 µL each of i5 and i7 Nextera XT indexing oligos (Illumina), and 3 µL of purified first-round PCR product. Thermal cycling conditions were as follows: 95°C for 3 min; followed by eight cycles of 95°C for 30 s, 55°C for 30 s and 72°C for 30 s; and finally, 72°C for 5 min. Following purification using 1× AMPure beads, DNA concentrations were measured with the Quant-iT PicoGreen dsDNA Assay Kit and amplicon libraries were pooled at equimolar concentration. The pooled library was supplemented with phiX DNA (30% final concentration) and sequenced on a MiSeq instrument using V2 chemistry (2 × 251 bp reads).

Data availability

All sequencing data have been deposited in NCBI's Sequence Read Archive repository under BioProject PRJNA715597.

Other method information

Reagents, measuring instruments and measurement parameters, sequencing data processing and analysis, and lipid data analysis are given in Supplementary Tables S17.

Declarations

Acknowledgments

The authors express their deepest gratitude to Keiko Nakai and Hiroyuki Ishii at LSI Medience Co. for their advice on the monkeys and their help in collecting the specimens. We thank Chiyo Morita and Ayako Kobayashi at the University of Tokyo, and Ryota Kato, Koudai Yamada, Kako Shimada, and Saki Akagi at

Kyoto Pharmaceutical University for technical assistance in several experiments. We are grateful to Daisuke Higo (Thermo Fisher Scientific K. K.) and Takefumi Moriya (Mitsui Knowledge Industry Co., Ltd.) for supporting our work. We are also deeply grateful to JMBC (Japan Microbiome Consortium) for their support of this research.

Author contributions

F. H. and S. M. T. took care of the samples, did the measurements, and found the importance of stool water content for lipids data analysis. M. I. performed metabolomic measurements and untargeted lipidome analysis, and Y. Y. was responsible for lipid identification and quantitative analysis from LC/MS data. DMT and YS were in charge of the microbiome, while Y. K. was responsible for lipid mediator analysis and lipid data management. H. Y. was in charge of trace element analysis, and T. S. and Y. O. supervised the entire study.

Additional Information

We declare that we have no known competing financial interests or personal relationships that could have appeared to influence the work reported in this paper.

Abbreviations

Lipid Abbreviations used in the article:

LPC: lysophosphatidylcholine, PC: phosphatidylcholine, LPE: lysophosphatidylethanolamine, PE: phosphatidylethanolamine, LPG: lysophosphatidylglycerol, PG: phosphatidylglycerol, PA: phosphatidic acid, Cer: Ceramides, CerP: Ceramides phosphate, HexCer: Hexosylceramide, Hex1Cer: Monohexosylceramide, Hex2Cer: Dihexosylceramides, Hex3Cer: Trihexosylceramide, SM: sphingomyelin, SPH: Sphingosine, DG: diglyceride, TG: triglyceride, dMePE: dimethylphosphatidylethanolamine, LdMePE: lysodimethylphosphatidylethanolamine, PEt: phosphatidylethanol, PMe: phosphatidylmethanol.

References

1. Phillips, K. A. *et al.* Why primate models matter. *Am. J. Primatol.* **76**, 801–827 (2014).
2. Colman, R. J. Non-human primates as a model for aging. *Biochim. Biophys. Acta - Mol. Basis Dis.* **1864**, 2733–2741 (2018).
3. Misra, B. B. *et al.* High-resolution gas chromatography/mass spectrometry metabolomics of non-human primate serum. *Rapid Commun. Mass Spectrom.* **32**, 1497–1506 (2018).
4. Hird, D. W., Anderson, J. H. & Bielitzki, J. T. Diarrhea in nonhuman primates: a survey of primate colonies for incidence rates and clinical opinion. *Lab. Anim. Sci.* **34**, 465–470 (1984).
5. Gottlieb, D. H. *et al.* Personality, environmental stressors, and diarrhea in Rhesus macaques: An interactionist perspective. *Am. J. Primatol.* **80**, 1–14 (2018).

6. Zhu, S. *et al.* Identification of Gut Microbiota and Metabolites Signature in Patients With Irritable Bowel Syndrome. *Front. Cell. Infect. Microbiol.* **9**, 1–12 (2019).
7. Liu, S. *et al.* Multi-omics Analysis of Gut Microbiota and Metabolites in Rats With Irritable Bowel Syndrome. *Front. Cell. Infect. Microbiol.* **9**, 178 (2019).
8. Zhang, W. X. *et al.* Altered profiles of fecal metabolites correlate with visceral hypersensitivity and may contribute to symptom severity of diarrhea-predominant irritable bowel syndrome. *World J. Gastroenterol.* **25**, 6416–6429 (2019).
9. Pinu, F. R. *et al.* Systems biology and multi-omics integration: Viewpoints from the metabolomics research community. *Metabolites.* **9**, 1–31 (2019).
10. Subramanian, I., Verma, S., Kumar, S., Jere, A. & Anamika, K. Multi-omics Data Integration, Interpretation, and Its Application. *Bioinform. Biol. Insights.* **14**, 7–9 (2020).
11. Lancaster, S. M., Sanghi, A., Wu, S. & Snyder, M. P. A customizable analysis flow in integrative multi-omics. *Biomolecules.* **10**, 1–15 (2020).
12. Wörheide, M. A., Krumsiek, J., Kastenmüller, G. & Arnold, M. Multi-omics integration in biomedical research – A metabolomics-centric review. *Anal. Chim. Acta.* **1141**, 144–162 (2021).
13. Bliss, D. Z. *et al.* Comparison of subjective classification of stool consistency and stool water content. *Journal of Wound, Ostomy and Continence Nursing.* **26**, 137–141 (1999).
14. Vandeputte, D. *et al.* Stool consistency is strongly associated with gut microbiota richness and composition, enterotypes and bacterial growth rates. *Gut.* **65**, 57–62 (2016).
15. Li, S. *et al.* Predicting Network Activity from High Throughput Metabolomics.*PLoS Comput. Biol.***9**, (2013).
16. Quell, J. D. *et al.* Automated pathway and reaction prediction facilitates in silico identification of unknown metabolites in human cohort studies. *J. Chromatogr. B Anal. Technol. Biomed. Life Sci.* **1071**, 58–67 (2017).
17. Cai, Q., Alvarez, J. A., Kang, J. & Yu, T. Network Marker Selection for Untargeted LC-MS Metabolomics Data. *J. Proteome Res.* **16**, 1261–1269 (2017).
18. Basu, S. *et al.* Sparse network modeling and metscape-based visualization methods for the analysis of large-scale metabolomics data. *Bioinformatics.* **33**, 1545–1553 (2017).
19. Wu, T. *et al.* Reliability of LipidSearch software identification and its application to assess the effect of dry salting on the long-chain free fatty acid profile of tilapia muscles. *Food Res. Int.* **138**, 109791 (2020).
20. Trzeciecka, A. *et al.* Comparative lipid profiling dataset of the inflammation-induced optic nerve regeneration.*Data Br.***24**, (2019).
21. Astarita, G., Kendall, A. C., Dennis, E. A. & Nicolaou, A. Targeted lipidomic strategies for oxygenated metabolites of polyunsaturated fatty acids. *Biochim. Biophys. Acta - Mol. Cell Biol. Lipids.* **1851**, 456–468 (2015).

22. Gabbs, M., Leng, S., Devassy, J. G. & Aukema, H. M. Advances in Our Understanding of Oxylipins Derived from Dietary PUFAs. *Am. Soc. Nutr.* **6**, 513–540 (2015).
23. Rohr, M., Narasimhulu, C. A., Keewan, E., Hamid, S. & Parthasarathy, S. The dietary peroxidized lipid, 13-HPODE, promotes intestinal inflammation by mediating granzyme B secretion from natural killer cells. *Food Funct.* **11**, 9526–9534 (2020).
24. Keewan, E., Narasimhulu, C. A., Rohr, M., Hamid, S. & Parthasarathy, S. Are fried foods unhealthy? The dietary peroxidized fatty acid, 13-hpode, induces intestinal inflammation in vitro and in vivo. *Antioxidants.* **9**, 1–17 (2020).
25. Brown, K. & Arthur, J. Selenium, selenoproteins and human health: a review. *Public Health Nutr.* **4**, 593–599 (2001).
26. Zoidis, E., Seremelis, I., Kontopoulos, N. & Danezis, G. P. Selenium-dependent antioxidant enzymes: Actions and properties of selenoproteins. *Antioxidants.* **7**, 1–26 (2018).
27. Kang, D. *et al.* The role of selenium metabolism and selenoproteins in cartilage homeostasis and arthropathies. *Exp. Mol. Med.* **52**, 1198–1208 (2020).
28. Takahashi, K., Suzuki, N. & Ogra, Y. Effect of gut microflora on nutritional availability of selenium. *Food Chem.* **319**, 1–8 (2020).
29. Vacca, M. *et al.* The controversial role of human gut lachnospiraceae. *Microorganisms.* **8**, 1–25 (2020).
30. Lee, G. *et al.* Distinct signatures of gut microbiome and metabolites associated with significant fibrosis in non-obese NAFLD. *Nat. Commun.* **11**, 1–13 (2020).
31. Liu, S. *et al.* Altered gut microbiota and short chain fatty acids in Chinese children with autism spectrum disorder. *Sci. Rep.* **9**, 1–9 (2019).
32. WATANABE, S. *et al.* A cross-sectional analysis from the Mykinso Cohort Study: establishing reference ranges for Japanese gut microbial indices. Biosci. Microbiota, Food Heal. advpub(2021).
33. Brunkwall, L., Ericson, U., Nilsson, P. M., Orho-Melander, M. & Ohlsson, B. Self-reported bowel symptoms are associated with differences in overall gut microbiota composition and enrichment of Blautia in a population-based cohort. *J. Gastroenterol. Hepatol.* **36**, 174–180 (2021).
34. Kaakoush, N. O. Insights into the role of Erysipelotrichaceae in the human host. *Front. Cell. Infect. Microbiol.* **5**, 1–4 (2015).
35. Nakajima, H. *et al.* The effects of metformin on the gut microbiota of patients with type 2 diabetes: A two-center, quasi-experimental study. *Life.* **10**, 1–15 (2020).
36. Schoster, A., Staempfli, H. R., Guardabassi, L. G., Jalali, M. & Weese, J. S. Comparison of the fecal bacterial microbiota of healthy and diarrheic foals at two and four weeks of life. *BMC Vet. Res.* **13**, 1–10 (2017).
37. Steffen, B. T. *et al.* Plasma omega-3 and saturated fatty acids are differentially related to pericardial adipose tissue volume across race/ethnicity: the Multi-ethnic Study of Atherosclerosis. *Eur. J. Clin. Nutr.* https://doi.org/10.1038/s41430-020-00833-x (2021).

38. Matura, S. *et al.* Association of dietary fat composition with cognitive performance and brain morphology in cognitively healthy individuals. *Acta Neuropsychiatr.* 1–23 https://doi.org/10.1017/neu.2021.1 (2021).
39. Bujtor, M. *et al.* Associations of dietary intake on biological markers of inflammation in children and adolescents: A systematic review. *Nutrients.* **13**, 1–29 (2021).
40. Zhao, L. *et al.* Saturated long-chain fatty acid-producing bacteria contribute to enhanced colonic motility in rats. *Microbiome.* **6**, 1–16 (2018).
41. Voshol, P. J., Rensen, P. C. N., van Dijk, K. W., Romijn, J. A. & Havekes, L. M. Effect of plasma triglyceride metabolism on lipid storage in adipose tissue: Studies using genetically engineered mouse models. *Biochim. Biophys. Acta - Mol. Cell Biol. Lipids.* **1791**, 479–485 (2009).
42. Ohtsu, H., Yakabe, Y., Yamazaki, M., Murakami, H. & Abe, H. Plasma lipid profiles and redox status are modulated in a ketogenic diet-induced chicken model of ketosis. *J. Poult. Sci.* **50**, 212–218 (2013).
43. Benjamin, B., Wada, Y., Grundy, S. M., Szuszkiewicz-Garcia, M. & Vega, G. L. Fatty acid oxidation in normotriglyceridemic men. *J. Clin. Lipidol.* **10**, 283–288 (2016).
44. Ma, C. *et al.* Upregulated ethanolamine phospholipid synthesis via selenoprotein I is required for effective metabolic reprogramming during T cell activation. *Mol. Metab.* **47**, 101170 (2021).
45. Cummings, R., Parinandi, N., Wang, L., Usatyuk, P. & Natarajan, V. Phospholipase D/phosphatidic acid signal transduction: role and physiological significance in lung. *Mol. Cell. Biochem.* **234–235**, 99–109 (2002).
46. Tappia, P. S., Dent, M. R. & Dhalla, N. S. Oxidative stress and redox regulation of phospholipase D in myocardial disease. *Free Radic. Biol. Med.* **41**, 349–361 (2006).
47. Ramrakhiani, L. & Chand, S. Recent progress on phospholipases: Different sources, assay methods, industrial potential and pathogenicity. *Appl. Biochem. Biotechnol.* **164**, 991–1022 (2011).
48. Isaksson, A., Walther, L., Hansson, T., Andersson, A. & Alling, C. Phosphatidylethanol in blood (B-PEth): A marker for alcohol use and abuse. *Drug Test. Anal.* **3**, 195–200 (2011).
49. Liu, J. J. *et al.* Profiling of Plasma Metabolites Suggests Altered Mitochondrial Fuel Usage and Remodeling of Sphingolipid Metabolism in Individuals With Type 2 Diabetes and Kidney Disease. *Kidney Int. Reports.* **2**, 470–480 (2017).
50. Bhat, O. M., Yuan, X., Li, G., Lee, R. & Li, P. L. Sphingolipids and redox signaling in renal regulation and chronic kidney diseases. *Antioxidants Redox Signal.* **28**, 1008–1026 (2018).
51. Wang, Y., Chen, Y., Zhang, X., Lu, Y. & Chen, H. New insights in intestinal oxidative stress damage and the health intervention effects of nutrients: A review. *J. Funct. Foods.* **75**, 104248 (2020).
52. Vona, R., Pallotta, L., Cappelletti, M., Severi, C. & Matarrese, P. The impact of oxidative stress in human pathology: Focus on gastrointestinal disorders. *Antioxidants.* **10**, 1–26 (2021).
53. Knuplez, E. & Marsche, G. An updated review of pro-and anti-inflammatory properties of plasma lysophosphatidylcholines in the vascular system. *Int. J. Mol. Sci.* **21**, 1–18 (2020).

54. Kita, Y., Takahashi, T., Uozumi, N. & Shimizu, T. A multiplex quantitation method for eicosanoids and platelet-activating factor using column-switching reversed-phase liquid chromatography-tandem mass spectrometry. *Anal. Biochem.* **342**, 134–143 (2005).

55. Parada, A. E., Needham, D. M. & Fuhrman, J. A. Every base matters: Assessing small subunit rRNA primers for marine microbiomes with mock communities, time series and global field samples. *Environ. Microbiol.* **18**, 1403–1414 (2016).

56. Apprill, A., Mcnally, S., Parsons, R. & Weber, L. Minor revision to V4 region SSU rRNA 806R gene primer greatly increases detection of SAR11 bacterioplankton. *Aquat. Microb. Ecol.* **75**, 129–137 (2015).

Supplementary Table S6

Supplementary Table S6 was not provided with this version of the manuscript.

Figures

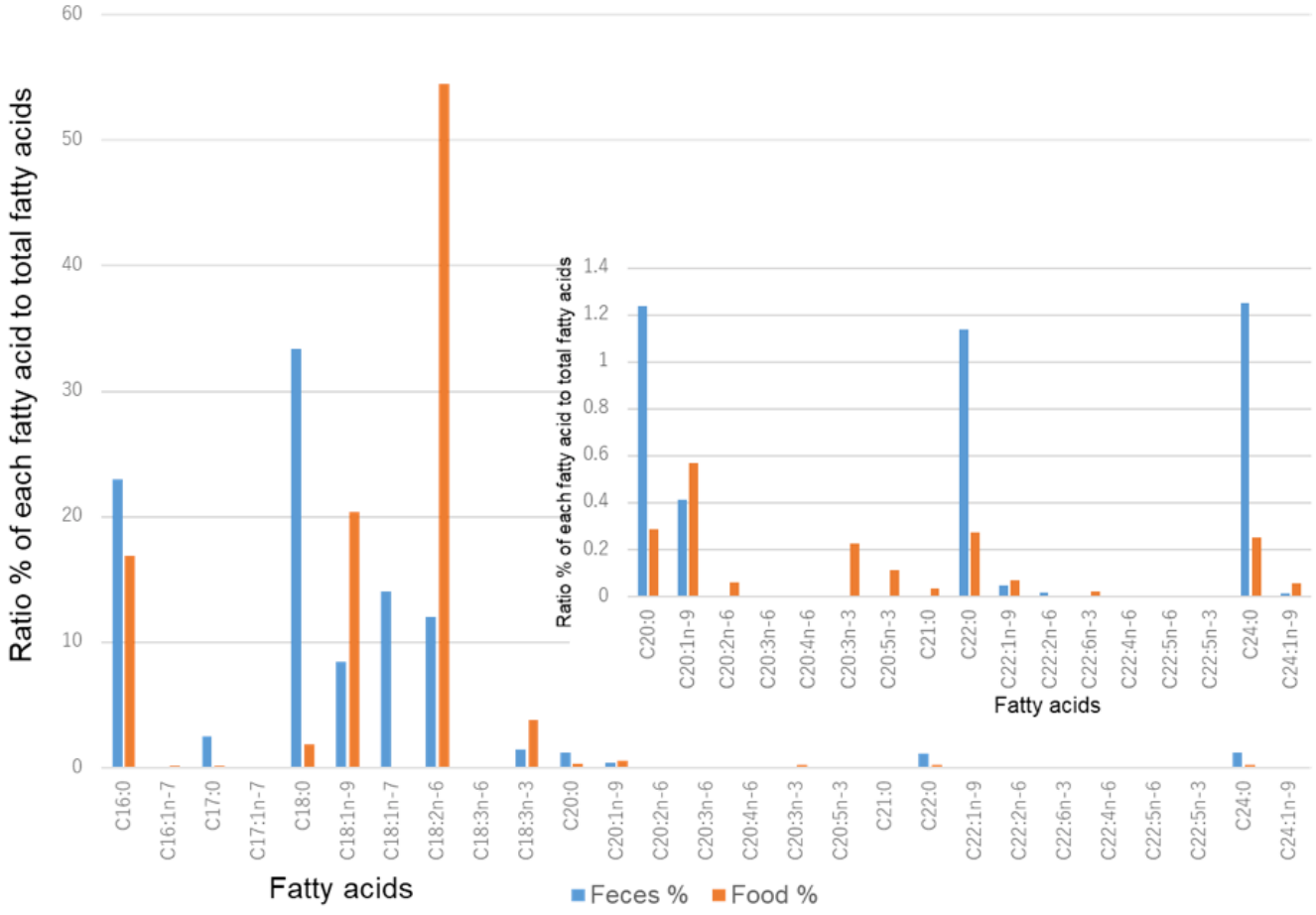

Figure 1

Figure 1

Comparison of fatty acid species in food and feces. The orange bars represent the fatty acids in the food, the blue bars the fatty acids in the feces, the vertical axis shows the percentage, when the total fatty acid content is 100%, and the horizontal axis shows the fatty acid species. The graph embedded in the figure is a magnified view of fatty acids with carbon chains of more than 20.

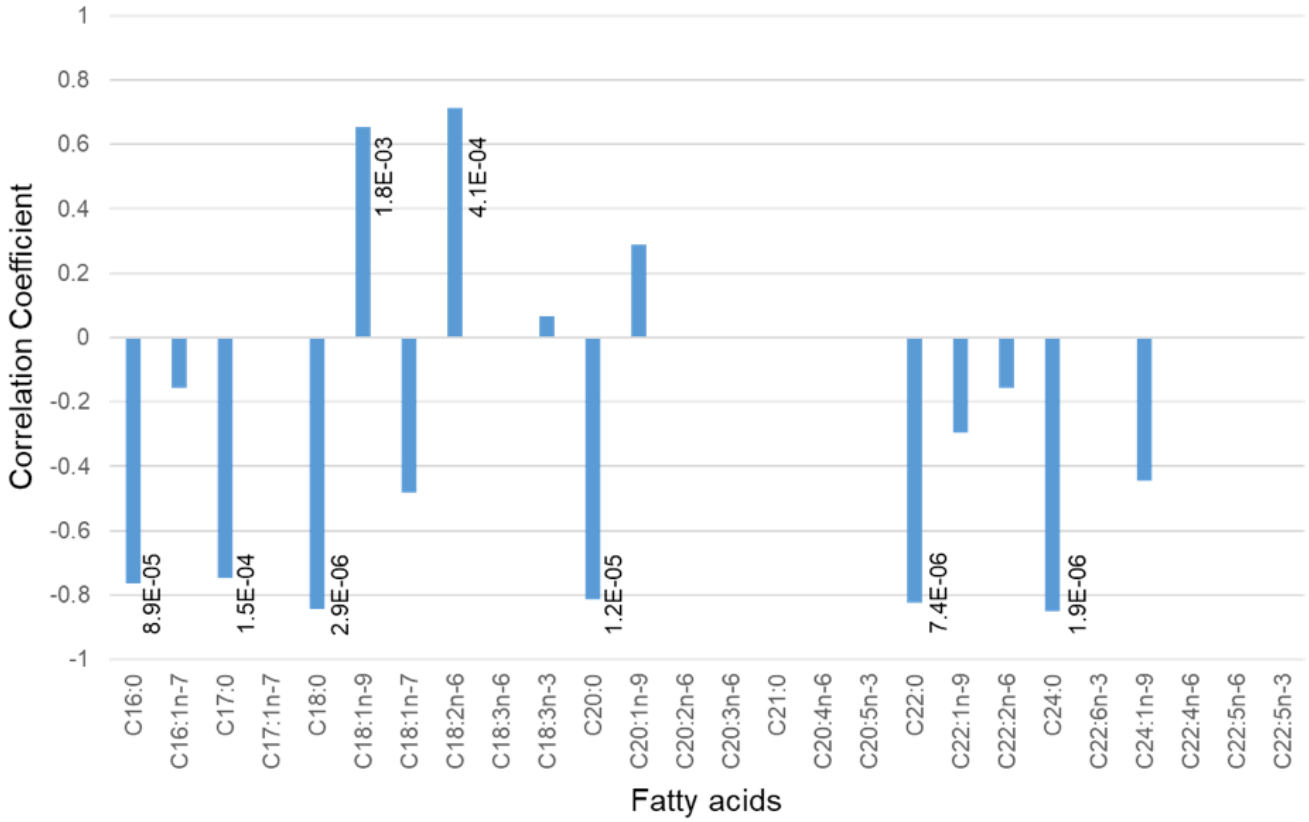

Figure 2

Figure 2

Correlation between water content and fatty acid content in feces. The correlation coefficient was calculated based on Pearson's correlation coefficient and was shown on the vertical axis. The horizontal axis shows the type of fatty acid: the number following the C indicates the length of the carbon chain, the number following the colon indicates the number of unsaturated bonds, and the number following the n- indicates the position of the first unsaturated bond counting from the position of the carbon atom of the terminal methyl group. The fatty acids were measured by GC after derivatization. The numbers next to the bar graph are the p-values.

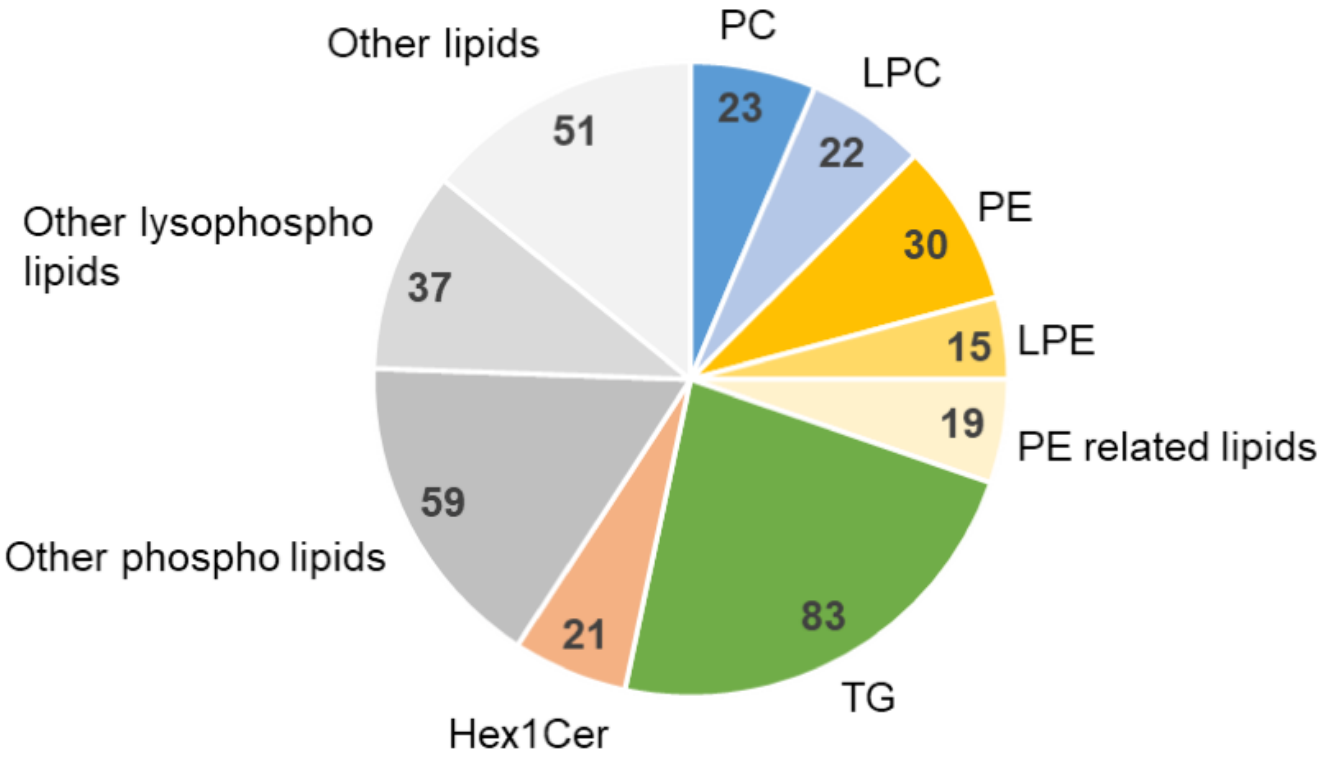

Figure 3

Figure 3

Lipidomics on monkey food. The numbers represent the number of lipids identified. PE related lipids are LdMePE (5 lipids) and dMePE (14 lipids). PC; phosphatidylcholine, LPC: lysophosphatidylcholine, PE: phosphatidylethanolamine, LPE: lysophosphatidylethanolamine, TG: triglyceride, Hex1Cer: Hexosylceramide.

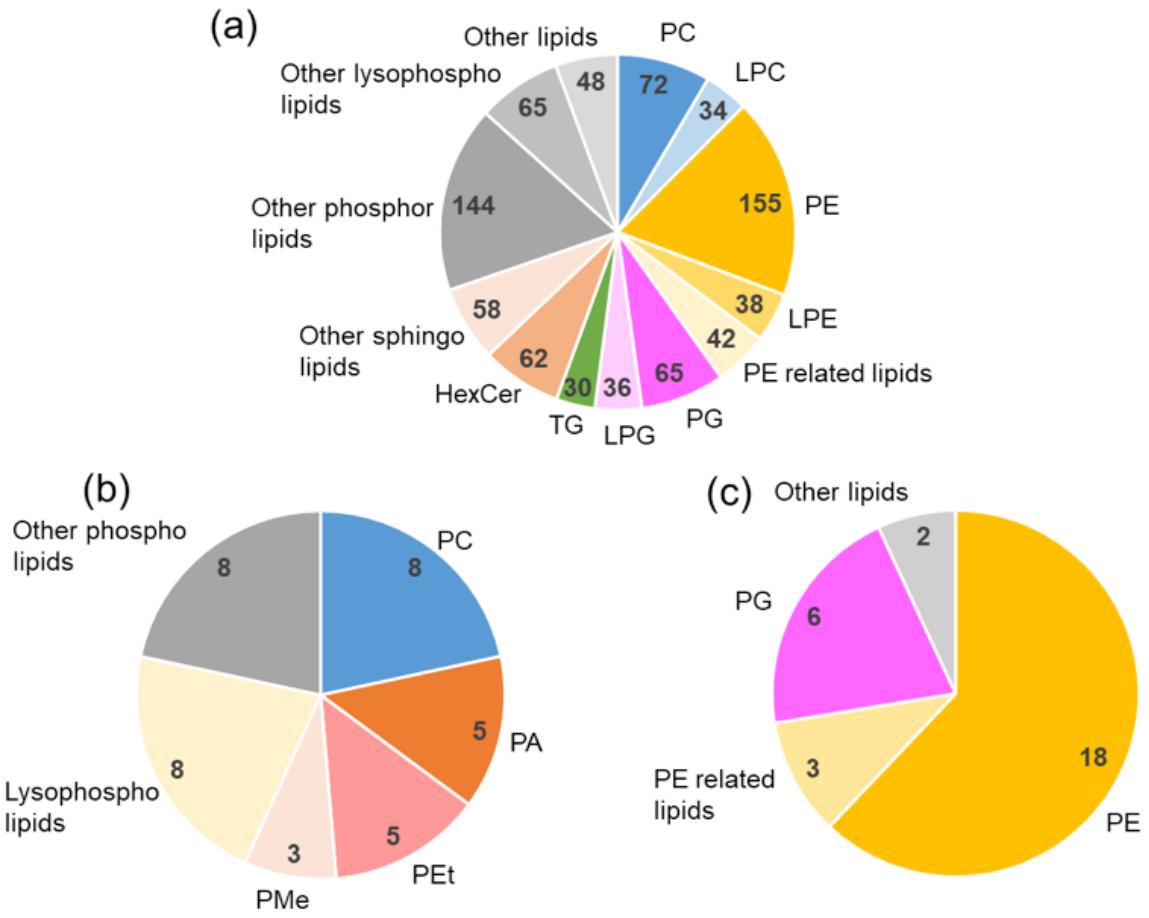

Figure 4

Figure 4

Fecal lipidomics. (a) Distribution of lipid components in the stool. (b) Lipids in stool with a significant positive correlation with stool water content. (c) Lipids in stool with significant negative correlation with stool water content. PC; phosphatidylcholine, LPC: lysophosphatidylcholine, PE: phosphatidylethanolamine, LPE: lysophosphatidylethanolamine, PG: phosphatidylglycerol, LPG: lysophosphatidylglycerol, TG: triglyceride, HexCer: Hexosylceramide, PA: phosphatidic acid, PEt: phosphatidylethanol, PMe: phosphatidylmethanol.

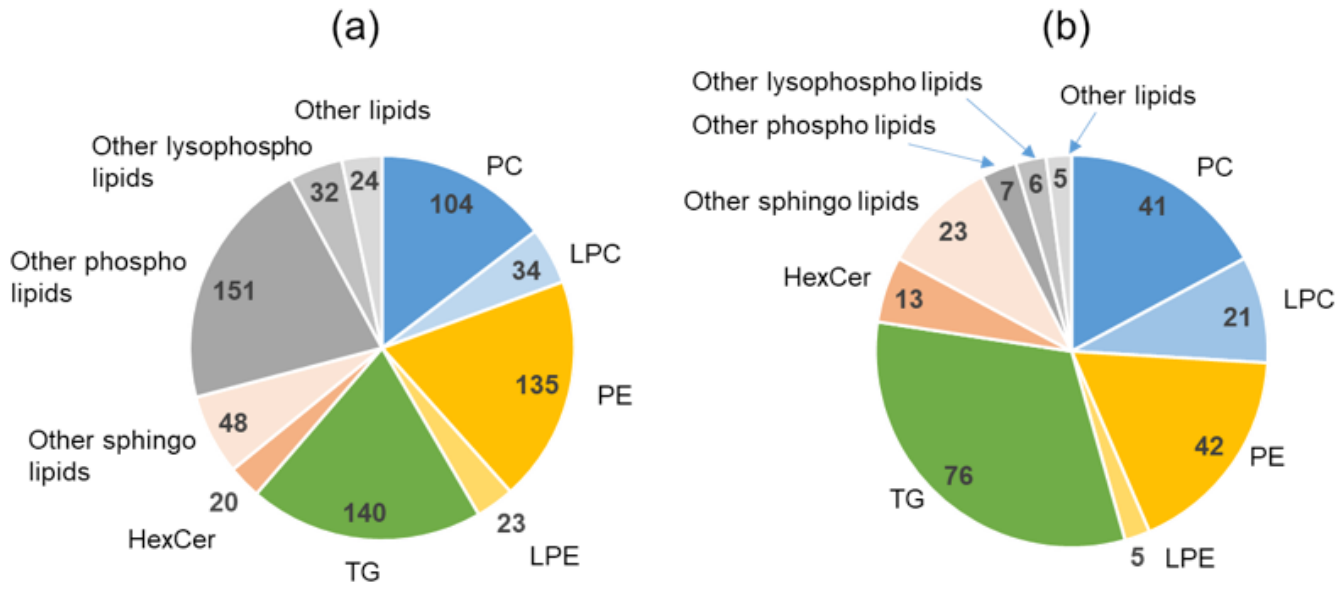

Figure 5

Figure 5

Plasma lipidomics. (a) Distribution of lipid components in the plasma. (b) Lipids in plasma with significant negative correlation with stool water content. PC; phosphatidylcholine, LPC: lysophosphatidylcholine, PE: phosphatidylethanolamine, LPE: lysophosphatidylethanolamine, TG: triglyceride, HexCer: Hexosylceramide.

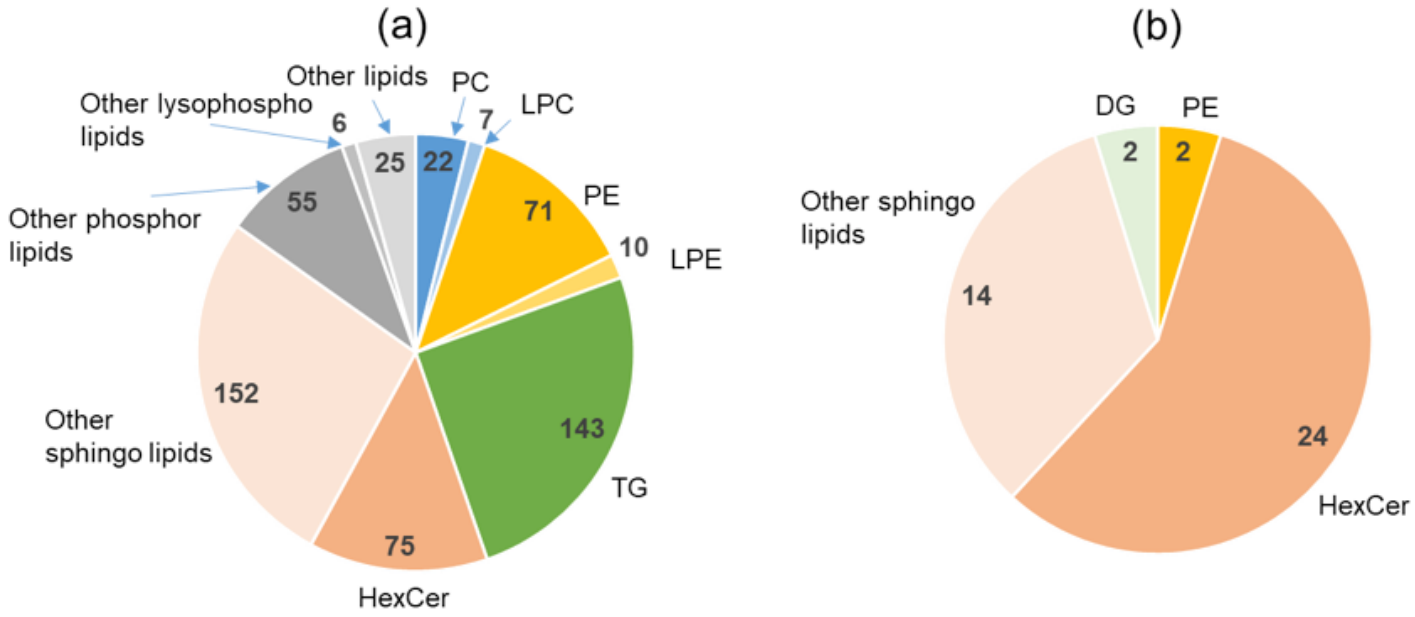

Figure 6

Figure 6

Urinary lipidomics. (a) Distribution of lipid components in the urine. (b) Lipids in urine with a significant positive correlation with stool water content. PC; phosphatidylcholine, LPC: lysophosphatidylcholine, PE: phosphatidylethanolamine, LPE: lysophosphatidylethanolamine, TG: triglyceride, HexCer: Hexosylceramide, DG: diglyceride.

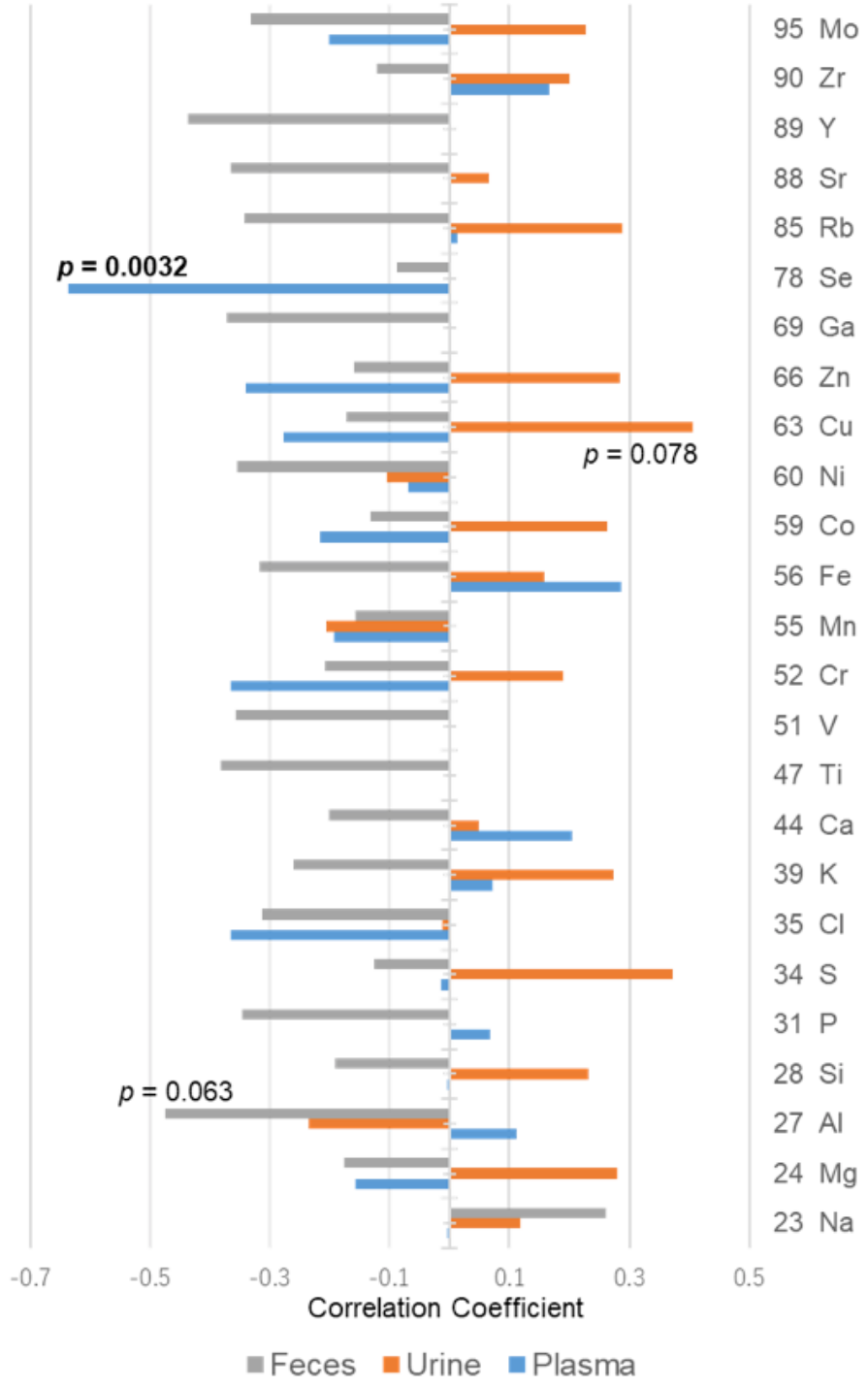

Figure 7

Figure 7

Correlation coefficient between trace elements in plasma, urine, or feces, and stool water content. The numbers next to the bar graph are the p-values. There were no significant differences ($p > 0.05$) except for the two mentioned on the graphs. Gray bars: feces samples; orange bars: urine samples; and blue bars: plasma samples.

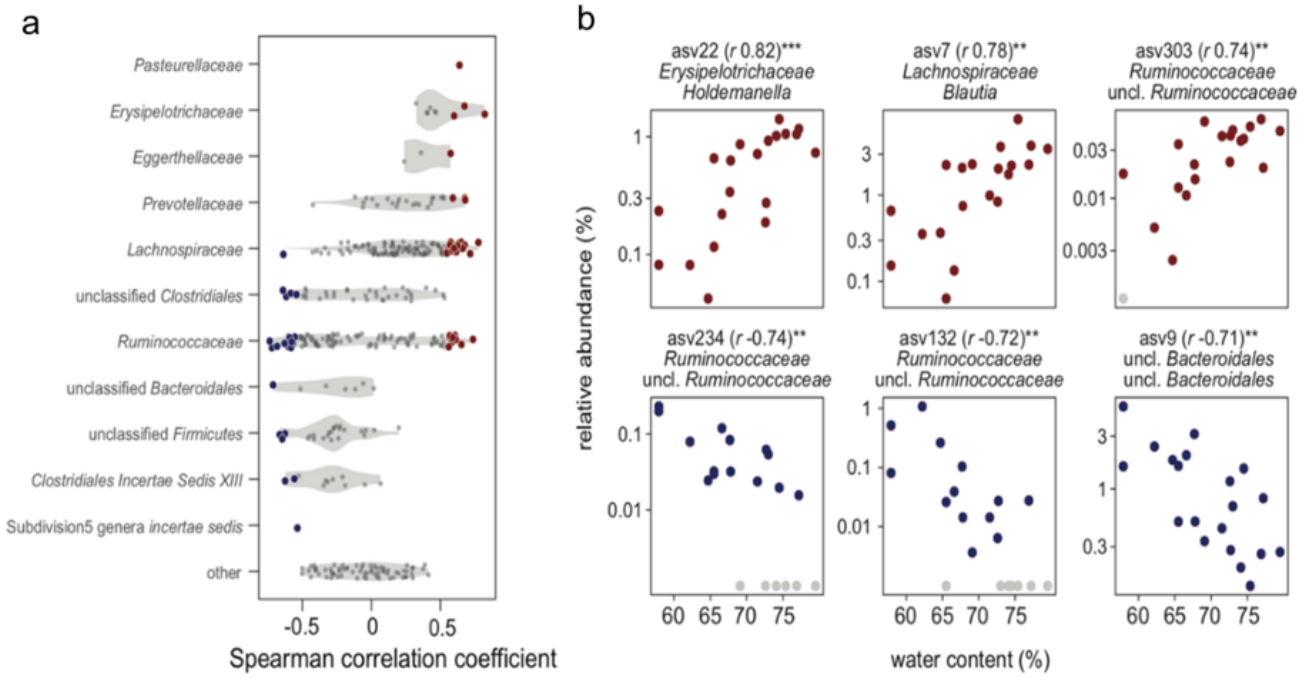

Figure 8

Figure 8

Fecal microbial diversity and their relation with fecal water content. (a) Summary of Spearman's correlation coefficients of the relationship between ASV abundance and water content. Violin plots show the distribution of correlation coefficients for all ASVs analyzed and grouped according to taxonomic affiliation (y-axis). Non-significant correlation coefficients (adjusted P-value threshold of 0.1) are shown as dark gray circles, and significant negative and positive correlations are plotted as blue and red circles, respectively. (b) Scatter plots of ASV abundance and water content for ASVs with the most significant positive (top) and negative (bottom) correlations (*** adjusted P-value of < 0.01 and ** adjusted P-value of <0.05). Graphics for all ASVs with significant correlations are shown in Supplementary Fig. S2. Note that ASVs with zero abundances in the rarified ASV tables are shown as light gray symbols, plotted at a pseudo-abundance of 0.001%.

Supplementary Files

This is a list of supplementary files associated with this preprint. Click to download.

- SupplementaryFiguresandTables.docx

- SupplTableS1Stoolwatercontent.xlsx
- SupplTableS2Plasmahydrophilic.xlsx
- SupplTableS3UrineHydophilic.xlsx
- SupplTableS4FecalHydrophilic.xlsx
- SupplTableS5HMDBFecesHydrophiric.xlsx
- SupplTableS7Foodlipidmics.xlsx
- SupplTableS8FecalLipidomics.xlsx
- SupplTableS9PlasmaLipidomics.xlsx
- SupplTableS10UrinaryLipidomics.xlsx
- SupplTableS11FecalOxidizedFattyacids.xlsx
- SupplTableS12PlasmaOxidizedFattyacids.xlsx
- SupplTableS13Oxidizedfattyacidsinfecesandstoolwatercontent.xlsx
- SupplTableS14UrinaryOxidizedFattyacids.xlsx
- SupplTableS15MetallomicsPlasmaFecesUrine.xlsx
- SupplTableS16FoodMetallomics.xlsx
- SupplementaryTablesS17.docx